Carbon-13 Chemical Shielding Parameters in Liquid Hexafluorobenzene Determined by NMR Relaxation Measurements

F. Guenneau,[†] P. Mutzenhardt,*[,†] X. Assfeld,[‡] and D. Canet[†]

Laboratoire de Méthodologie RMN, UPRESA 7042, Université Henri Poincaré, Nancy I, BP.239, 54506 Vandoeuvre-lès-Nancy (Cedex), France, and Laboratoire de Chimie Théorique de Nancy, UMR 7565, Université Henri Poincaré, Nancy I, BP.239, 54506 Vandoeuvre-lès-Nancy (Cedex), France

Received: June 19, 1998

Simple pulse sequences have been used to determine and isolate most carbon-13 and fluorine-19 longitudinal relaxation parameters in pure hexafluorobenzene (carbon-13 in natural abundance). The derived parameters include fluorine-19 and carbon-13 specific relaxation rates (at different field values), dipolar fluorine-carbon cross-relaxation rate, and dipolar (^{13}C−^{19}F)-chemical shift anisotropy (^{13}C or ^{19}F) cross-correlation rates. From these experimental parameters, it was possible to estimate the reorientational anisotropy of liquid hexafluorobenzene and to extract the shielding tensor elements of fluorine-19 and carbon-13. Comparison with those elements as determined from solid-state NMR shows a good agreement for fluorine-19 but one important difference (for one element) in the carbon-13 shielding tensor. This feature is confirmed by quantum chemistry calculations and can be explained by the particular ordering in pure solid.

Introduction

Although chemical shift anisotropy (CSA) effects can be determined in solid-state NMR spectra, the rapid molecular reorientation in the liquid phase provides only a direct measurement of the isotropic shift, i.e., one-third of the trace of the chemical shielding tensor. Nevertheless, CSA affects spin relaxation in a general way and can interfere with the dipolar interaction mechanism.[1−3] The resulting process named cross-correlation is generally measured by observing its effects on longitudinal relaxation[4−7] and can also be reliably measured through transverse relaxation as demonstrated in recent papers.[8,9] Previously we have studied the molecular reorientation of pure liquid benzene[10] using carbon-13 shielding parameters deduced from solid-state NMR data. The scope of this paper is an extension of this methodology in order to determine also shielding parameters. One of the reason for which benzene and its derivatives have been the subject of numerous studies in solid and liquid phases is that they form molecular complexes. The case of hexafluorobenzene is particularly appealing because an important variation of the isotropic shift of about 20 ppm occurs upon going from pure solid to liquid or to liquid mixtures or even to solid mixtures. To the best of our knowledge the carbon-13 shielding tensor of hexafluorobenzene has not been measured in the liquid state, and this led us, with appropriate NMR experiments and reliable quantum chemistry calculations, to attempt to determine this quantity and discuss the unusual behavior of the carbon-13 isotropic shift.

Theory

Although dipolar fluorine−fluorine and remote fluorine−carbon interactions provide non-negligible relaxation mechanisms, the simplifying assumption of an isolated ^{19}F−^{13}C pair will be considered first and a posteriori justified. A detailed theoretical report along with methodological aspects related to the present study has already been presented in a previous paper devoted to the reorientational anisotropy of benzene[10] and will therefore be summarized here. The starting point is the well-known Solomon equations for a two-spin system, which are extended to account for the cross-correlation effect between the CSA relaxation and the dipolar relaxation mechanisms:[11]

$$\begin{aligned}
\frac{\mathrm{d}}{\mathrm{d}t}I_z^{\mathrm{C}} &= -R_1^{\mathrm{C}}(I_z^{\mathrm{C}} - I_{\mathrm{eq}}^{\mathrm{C}}) - \sigma_{\mathrm{CF}}(I_z^{\mathrm{F}} - I_{\mathrm{eq}}^{\mathrm{F}}) - \sigma_{\mathrm{CSA(C),d}}(2I_z^{\mathrm{C}}\, I_z^{\mathrm{F}}) \\
\frac{\mathrm{d}}{\mathrm{d}t}I_z^{\mathrm{F}} &= -R_1^{\mathrm{F}}(I_z^{\mathrm{F}} - I_{\mathrm{eq}}^{\mathrm{F}}) - \sigma_{\mathrm{CF}}(I_z^{\mathrm{C}} - I_{\mathrm{eq}}^{\mathrm{C}}) - \sigma_{\mathrm{CSA(F),d}}(2I_z^{\mathrm{C}}\, I_z^{\mathrm{F}}) \quad (1) \\
\frac{\mathrm{d}}{\mathrm{d}t}(2I_z^{\mathrm{C}}\, I_z^{\mathrm{F}}) &= -R_1^{\mathrm{CF}}(2I_z^{\mathrm{C}}\, I_z^{\mathrm{F}}) - \sigma_{\mathrm{CSA(C),d}}(I_z^{\mathrm{C}} - I_{\mathrm{eq}}^{\mathrm{C}}) - \\
&\qquad \sigma_{\mathrm{CSA(F),d}}(I_z^{\mathrm{F}} - I_{\mathrm{eq}}^{\mathrm{F}})
\end{aligned}$$

Each longitudinal magnetization is denoted by I_z^{X} with the superscript X being F for fluorine-19 or C for carbon-13 whereas $2I_z^{\mathrm{C}}\, I_z^{\mathrm{F}}$ stands for the so-called longitudinal spin order. Their corresponding equilibrium magnetizations and their longitudinal relaxation rates are denoted by $I_{\mathrm{eq}}^{\mathrm{X}}$ and R_1^{X}, respectively; $2I_z^{\mathrm{C}}\, I_z^{\mathrm{F}}$ is zero at thermal equilibrium. The two longitudinal magnetizations are coupled by cross-relaxation whereas cross-correlation (the interference CSA-dipolar terms) couples longitudinal magnetization and longitudinal spin order. The description of the hexafluorobenzene reorientation requires only two correlation times: $\tau_\perp$ associated with the tumbling of the symmetry axis perpendicular to the molecular plane and $\tau_\parallel$ associated with the rotation around this axis (Figure 1). These two dynamical parameters are involved in the longitudinal relaxation, dipolar cross-relaxation, and CSA-dipolar cross-correlation rates through the following expressions, valid in extreme narrowing conditions, satisfied here. For the dipolar cross-relaxation rate one

[†] Laboratoire de Méthodologie RMN.
[‡] Laboratoire de Chimie Théorique de Nancy.

S1089-5639(98)02697-8 CCC: $15.00 © 1998 American Chemical Society
Published on Web 08/14/1998

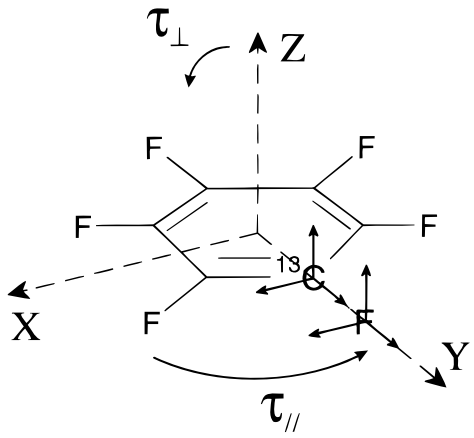

Figure 1. Molecular axis system *XYZ* and the principal axis system for the carbon-13 and fluorine-19 shielding tensors (displayed at the level of each atom), which are all coincident for symmetry reasons. The *X*, *Y*, *Z* labeling is consistent for each tensor with the usual convention $|\sigma_{zz}| \geq |\sigma_{yy}| \geq |\sigma_{xx}|$. This has been determined from solid-state NMR for fluorine and from quantum chemistry for carbon. The relevant rotational motion is schematized for each correlation time.

has

$$\sigma_{CF} = (1/2)(\mu_0/4\pi)^2(\gamma_C\gamma_F\hbar/r_{CF}^3)^2\tau_i \quad (2)$$

where r_{CF} stands for the bond length and τ_i is an effective correlation time related to the reorientation of the in-plane vector CF

$$\tau_i = \frac{1}{4}\left(\tau_\perp + 9\frac{\tau_\perp\tau_{||}}{2\tau_\perp + \tau_{||}}\right) \quad (3)$$

All other symbols have their usual meaning.

Because of the symmetry in the hexaflurobenzene molecule, the CF vector can be assumed to be collinear to one of the principal axes of the fluorine-19 or carbon-13 chemical shift tensors (see Figure 1). This yields the following expressions for the CSA-dipolar cross-correlation rates:

$$\sigma_{CSA(C),d} = (1/2)(\mu_0/4\pi)^2(\gamma_C\gamma_F\hbar/r_{CF}^3)\gamma_C B_0\Delta\sigma_C\tau_{CSA(C),d} \quad (4)$$

$$\sigma_{CSA(F),d} = (1/2)(\mu_0/4\pi)^2(\gamma_C\gamma_F\hbar/r_{CF}^3)\gamma_F B_0\Delta\sigma_F\tau_{CSA(F),d} \quad (4')$$

B_0 is the static magnetic field value and $\Delta\sigma_{C,F}$ represents either the carbon or the fluorine shielding anisotropy defined as $\Delta\sigma = \sigma_{zz} - (\sigma_{xx} + \sigma_{yy})/2$ (*x*, *y*, *z*: principal axes of the molecular shielding tensor with $|\sigma_{zz}| \geq |\sigma_{yy}| \geq |\sigma_{xx}|$; the same axis system turns out to be valid for carbon and fluorine nuclei). $\tau_{CSA(C),d}$ and $\tau_{CSA(F),d}$ are effective correlation times that depend on the shielding asymmetry parameters $\eta_{CSA(C)}$ and $\eta_{CSA(F)}$; the latter is defined as $(3/2)(\sigma_{yy} - \sigma_{xx})/\Delta\sigma$. Denoting by $\chi = \tau_\perp/\tau_{||}$ the reorientation anisotropy parameter and X referring either to carbon-13 or fluorine-19, we can express these effective correlation times as:

$$\tau_{CSA(X),d} = \frac{1 + 3\eta_{CSA(X)} + 2\chi}{1 + 2\chi}\tau_\perp \quad (5)$$

Longitudinal relaxation rates involve different contributions arising mainly from intramolecular and intermolecular dipole−dipole interactions and from the anisotropic nuclear shielding tensor, both modulated by molecular motion. The only magnetic field dependent mechanism is the one coming from CSA; its contribution to the longitudinal relaxation of each nucleus is of the form

$$R_1^{CSA(X)} = (2/15)(B_0\gamma_X\Delta\sigma_X)^2\tau_{CSA(X)} \quad (6)$$

where $\tau_{CSA(X)}$ is an effective correlation time that can be written as

$$\tau_{CSA(X)} = \left(\frac{1 + \eta_{CSA(X)}^2 + 2\chi}{1 + 2\chi}\right)\tau_\perp \quad (7)$$

On the other hand, the specific longitudinal relaxation rate for the two-spin order can be decomposed according to the other relaxation parameters[10]

$$R_1^{CF} = R_1^F + R_1^C - \frac{14}{5}\sigma_{CF} \quad (8)$$

Setting up an appropriate strategy for measuring the six relaxation rates involved in eqs 1 (possibly, for some of them, at different magnetic fields) could hopefully lead to the characterization of hexafluorobenzene molecular reorientation ($\tau_\perp$ and $\tau_{||}$) and to some pieces of information about carbon and fluorine shielding tensors.

Measurement of Relaxation Rates

Chemicals purchased from Aldrich and Fluka were of the highest available quality and were used without further purification. An NMR 5 mm o.d. sample tube, containing pure hexafluorobenzene with 2% v/v of hexadeuterobenzene added for field-frequency locking purpose, was carefully degassed by a sequence of "freeze−pump−thaw" cycles; the liquid being frozen, the tube was subsequently sealed under vacuum. All experiments were carried out at 25 °C. Longitudinal carbon and fluorine relaxation rates were measured at different fields: 2.1 and 4.7 T with home-made spectrometers, 7.04 T with an Avance Bruker DSX spectrometer, 9.4 T with an Avance Bruker DRX spectrometer, and 14.1 T with an Unity Varian spectrometer. Cross-relaxation and cross-correlation experiments were only performed at a field value of 9.4 T.

Longitudinal relaxation rates of fluorine-19 were obtained by means of the saturation-recovery experiment[12] at high field ($B_0 > 3$ T), which was preferred to the classical inversion-recovery experiment[13] owing to the necessity of avoiding radiation damping effects. Carbon-13 longitudinal relaxation rates were measured using both the fast inversion-recovery and the super fast inversion recovery[14] methods. Because of the small influence of the carbon CSA relaxation mechanism and of the required accuracy, all T_1 carbon-13 measurements were repeated (at least five times) for each magnetic field value.

The pulse sequence sketched in Figure 2 is designed for measuring the sole cross-relaxation rate associated with the dipolar interaction between directly bonded carbon-13 and fluorine-19 and therefore fulfills the assumption of an isolated pair of spins. For a detailed description of this experiment, the reader is referred to a previous work,[10] the important feature being that it is derived from the X-filtered HOESY experiments.[15] A typical experimental build-up curve is shown in Figure 3. In the same work we used an experiment (Figure 4) aimed at measuring the spin order longitudinal relaxation rate and one of the CSA-dipolar interference terms, depending on the observed nucleus. Assuming that the considered nucleus (carbon-13 in the following) is set on-resonance, we can see that, at the end of the interval of duration $1/2J_{CF}$, an antiphase configuration exists; it can be represented by $2I_x^C I_z^F$ and is converted by the next $(\pi/2)_{\pm y}$ pulse into longitudinal spin order,

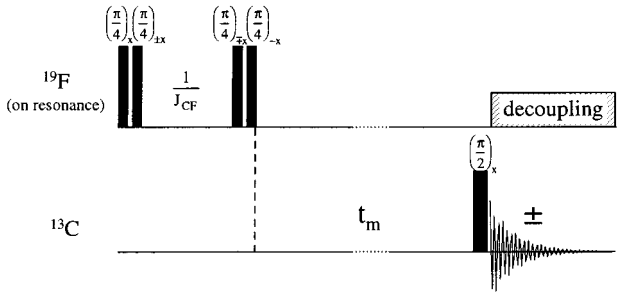

Figure 2. Pulse sequence used to measure selectively the cross-relaxation rates between directly bonded fluorine-19 and carbon-13. The spectrometer carrier frequency is set at the resonance of the fluorine-19 bonded to carbon-13 (average of the satellite frequencies) so that the heteronuclear coupling governs exclusively the evolution during the interval $1/J_{CF}$. The first step of the phase cycle inverts selectively fluorine bonded to carbon-13 while, during the second step, fluorine is not perturbed and the corresponding result serves as a reference.

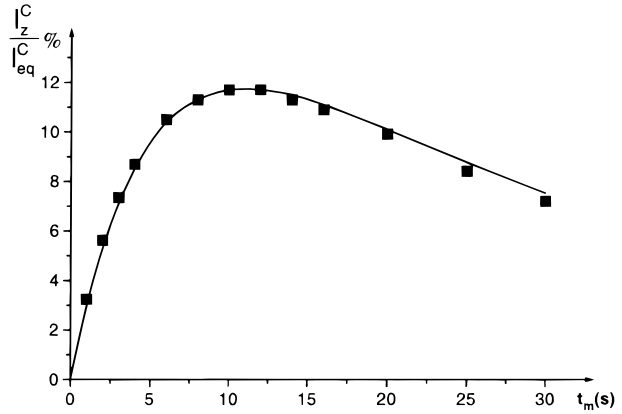

Figure 3. Typical build-up curve obtained from the experiment of Figure 2. Squares represent the experimental data, and the curve (solid line) has been recalculated from the fitted parameters. Experimental parameters used at 9.4T: 32 scans; recovery time, 300 seconds; acquisition, 16K complex data points for a spectral width of 1000 Hz. An exponential broadening of 2 Hz and one zero filling were applied before Fourier transformation.

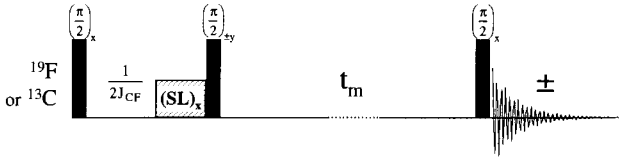

Figure 4. Pulse sequence used to measure the relaxation of the longitudinal spin order. The spin lock (SL) pulse purges out all unwanted magnetization. See text for other details.

$\pm 2I_z^C I_z^F$. During the mixing time t_m the longitudinal spin order decays according to its specific relaxation rate. The last ($\pi/2$) pulse acts as a read pulse and converts the longitudinal spin order back into an observable antiphase configuration. Phase cycling removes the carbon-13 longitudinal magnetization, which would reconstruct through its specific relaxation, while carbon-13 and fluorine-19 longitudinal magnetizations resulting from the CSA-dipolar cross-correlation terms are preserved. Transferred carbon-13 magnetization is thus edited through the last pulse of the sequence and normally yields a pure in-phase configuration superimposed to the antiphase, which arises from the longitudinal spin order. In the case of hexafluorobenzene, it was impossible to extract unambiguously this contribution from experimental data. The reason is that during the evolution delay $1/2J_{CF}$, and due to the complexity of the spin system,

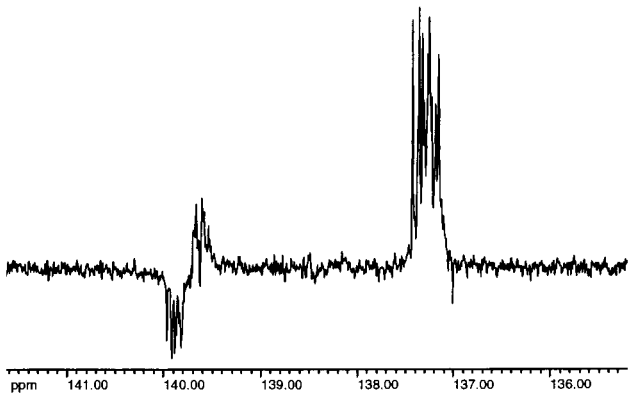

Figure 5. Data recorded with the experiment of Figure 4 for a null mixing time. A symmetric antiphase doublet was expected. Presumably, the creation of multiple quantum coherences during the evolution delay leads the complex pattern in the left part of the doublet, which precludes an accurate measurement of the CSA-dipolar cross-correlation term. Same experimental parameters as for Figure 3.

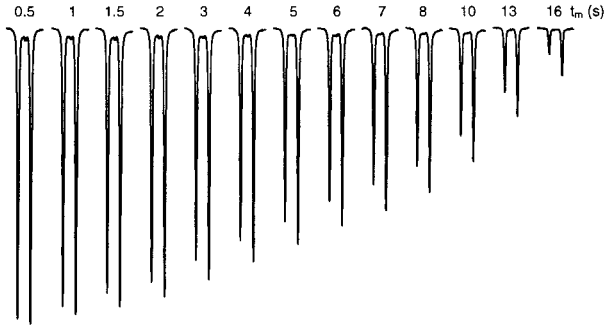

Figure 6. Spectra resulting from a simple inversion-recovery experiment applied to carbon-13 without fluorine-19 decoupling as a function of the mixing time t_m. A 20 Hz line broadening has been used to remove all the small splittings and to emphasize the intensity difference of the two remaining lines in the carbon-13 spectrum. Creation of the longitudinal spin order can be appreciated by the doublet asymmetry as the mixing time is increasing. Number of scans, 64; recovery time, 300 s; acquisition, 16K complex data points for a spectral width of 1000 Hz. One zero filling was applied before Fourier transformation.

other coherences are created that will survive the phase cycling. An example of what happens is shown in Figure 5. The main antiphase configuration arises, as expected, from the longitudinal spin order that was created at the beginning of the mixing time whereas an unexpected antiphase configuration is seen to be present in the left part of the doublet. This phenomenon is certainly interesting by itself but is beyond the scope of this article. In order to circumvent these difficulties we preferred to rely on two classical experiments that do not include transverse magnetization evolution.

The simplest is a carbon-13 inversion-recovery experiment without fluorine decoupling. It starts with the inversion of the carbon-13 magnetization, which subsequently recovers to its equilibrium value during the mixing time; this magnetization may be partly converted into longitudinal spin order by way of the dipolar (^{13}C−^{19}F)-CSA(^{13}C) cross-correlation mechanism. The last ($\pi/2$) pulse reads any kind of longitudinal magnetization including the longitudinal spin order, which appears in the form of an antiphase doublet superimposed to the in-phase doublet arising from the inverted normal longitudinal carbon-13 magnetization. The experimental results, presented in Figure 6, exhibit nonequal intensities for the two doublet components; this indicates an antiphase contribution originating from the longitudinal spin order. Theoretically this experiment could be used for each nucleus, but, in practice, it proved difficult to

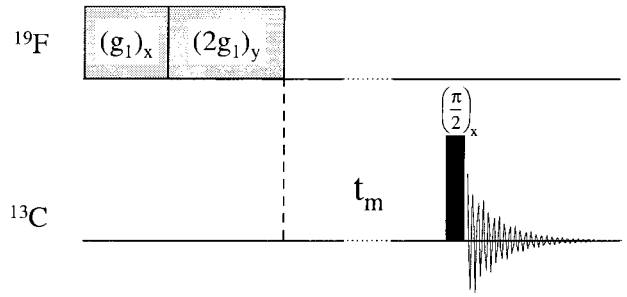

Figure 7. Pulse sequence used to measure the dipolar ($^{19}F-^{13}C$)-CSA(^{19}F) cross-correlation rate. A total saturation of the fluorine spin system is obtained by way of two high-power B_1 gradient pulses of 1.5 and 3 ms duration, respectively. During the mixing time both cross-relaxation and cross-correlation occur. The last pulse reads the state of any longitudinal magnetization.

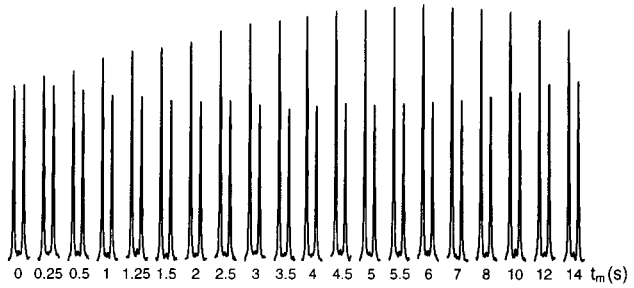

Figure 8. Data recorded with the experiment of Figure 7 (same conditions as for Figure 6). The creation of the longitudinal spin order can be followed (as a function of the mixing time) by the ^{13}C doublet asymmetry. The overall intensity increase is due to $^{19}F-^{13}C$ cross-relaxation.

obtain reliable fluorine-19 data. This is due to the huge central peak corresponding to fluorines bonded to carbon-12, which impairs the accurate quantification of the two small and largely splitted doublet components (corresponding to fluorines bonded to natural abundance carbon-13). Existing methods[16] could be used so as to remove this central line, but, as they involve free precession intervals, they must be avoided here for the reasons mentioned above. A solution to this problem consists of observing the carbon-13 magnetization after a complete saturation of the fluorine spin system (Figure 7). This sequence starts with two long B_1 gradient pulses delivered by a specific coil,[17] which completely defocus the fluorine magnetization. Thus (i) the initial fluorine magnetization state is perfectly known and is zero, (ii) during the mixing time, the carbon-13 magnetization will evolve from equilibrium via the dipolar cross-relaxation term and longitudinal spin order can be created by the dipolar ($^{13}C-^{19}F$)-CSA(^{19}F) interference mechanism. As in the previous experiment the last ($\pi/2$) pulse reads the state of any longitudinal magnetization but here at the carbon frequency without the aforementioned drawbacks. The experimental data are shown in Figure 8. Again, inequality in the doublet intensities assesses the creation of the longitudinal spin order by way of the dipolar ($^{13}C-^{19}F$)-CSA(^{19}F) cross-correlation mechanism. At this point, we possess relevant and reliable methods to measure the whole set of relaxation rates that governs eqs 1.

Quantum Chemistry Calculations

For the past several years, calculation of nuclear magnetic shielding constants has become an increasingly popular area for quantum chemical applications.[18] From the several contributions on this topic, one can elaborate a strategy to obtain quite accurate results (some ppm). If for most chemical systems the Hartree−Fock approximation gives suitable results, there are some cases that require to take into account electron correlation effects.[19] Moreover, it is well-known that values for the shielding tensor appear to be very sensitive to basis set size effects and to the geometry employed. In order to fulfill these three requirements (inclusion of the electronic correlation, basis set near the limit of completeness, and a reliable geometry), we decide to use the CC-PVTZ[20] basis set. This basis set, well-adapted to the treatment of correlation, is quite large (360 basis functions for the C_6F_6 molecule) and is expected to give results near the basis set limit. Inclusion of the electronic correlation can be done in many ways (MBPT, MCSCF, CCSD, ...), but methods based on density functional theory (DFT) are by far the cheapest with respect to computer time. At the present time DFT methods are the only one affordable for a system as large as C_6F_6 with our computer facilities. DFT potentials give accurate results for systems in the ground state and at the equilibrium geometry, in particular when nonlocal electronic density effects are included. However, since many functionals exist, we try some combination of exchange (B and B3)[21,22] and correlation (LYP and PW91)[23,24] functionals to examine their influence on the shielding tensor. Opposed to the Hartree−Fock-based methods, it is not possible to grade the level of theory of these functionals. Also, to the best of our knowledge, no systematic study has been performed to test the performance of various functionals to reproduce experimental shielding tensor. It is then a priori impossible to distinguish which calculation will be the best. Moreover, from the variety of theories available to compute shielding tensors, we decided to adopt the gauge including atomic orbital (GIAO) method[25] for the numerous advantages it presents,[26] and, in addition, methods developed by Bader et al., CSGT and IGAIM,[27] were considered. All calculations were carried out with the Gaussian-94 package.[28]

TABLE 1: Chemical Shielding Tensor Parameters (ppm) of Fluorine-19 and Carbon-13 at Various Levels of Theory

	C			F		
	σ_{xx}	σ_{yy}	σ_{zz}	σ_{xx}	σ_{yy}	σ_{zz}
GIAO-B3LYP	2.32	12.56	95.34	279.47	285.12	460.86
CSGT-B3LYP	5.41	13.53	95.64	267.48	285.99	453.45
IGAIM-B3LYP	5.41	13.53	95.64	267.48	285.99	453.45
GIAO-BLYP	6.43	7.17	88.73	258.93	272.09	455.87
GIAO-B3PW91	6.53	17.55	98.53	278.24	282.61	460.50
GIAO-BPW91	11.56	13.55	92.81	257.39	269.52	455.24

To check the reliability of our procedure, we compared the equilibrium geometry parameters obtained at the B3LYP and at the MP2 (full electrons) levels. Differences in the C−C and in the C−F bond lengths are found to be 0.008 and 0.004 Å, respectively, which are negligible for our purpose. Thus the working geometry is the one optimized at the B3LYP/CC-PVTZ level of theory.

It can be seen, from the results (Table 1 and 2), that all eigenvalues of the carbon atom shielding tensor are close to one another within a range that is less than 10 ppm (20 ppm for the fluorine atom). These discrepancies decrease significantly in the calculation of the parameters σ_{iso}, $\Delta\sigma$, and η, owing to average cancellation (ranges of about 6 ppm for carbon and 13 ppm for fluorine). The fact that both CSGT and IGAIM methods give the same results (truncated after the second digit!) indicate that the first-order current density distribution is adequate to describe outside the atomic bassin even though the gauge origin is coincident with the nucleus of the atom.

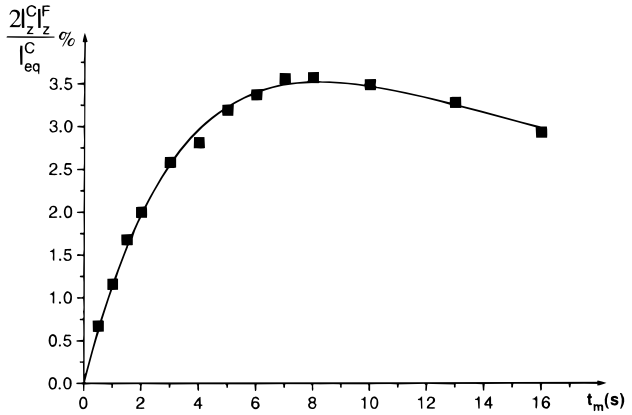

Figure 9. Typical build-up curve obtained by subtraction of the intensities of the two doublet components (data shown in Figure 6). The curve was fitted (solid line) according to eqs 1 and yields the dipolar (^{19}F−^{13}C)-CSA(^{13}C) cross-correlation rate.

TABLE 2: Chemical Shielding Asymmetry and Anisotropy of Fluorine-19 and Carbon-13 Deduced from Table 1

	C			F		
	σ_{iso} (ppm)	$\Delta\sigma$ (ppm)	η	σ_{iso} (ppm)	$\Delta\sigma$ (ppm)	η
GIAO-B3LYP	36.74	87.90	0.175	341.82	178.56	0.047
CSGT-B3LYP	38.19	86.17	0.141	335.64	176.72	0.157
IGAIM-B3LYP	38.19	86.17	0.141	335.64	176.72	0.157
GIAO-BLYP	34.11	81.93	0.014	328.96	190.37	0.104
GIAO-B3PW91	40.87	86.49	0.191	340.45	180.07	0.036
GIAO-BPW91	39.30	80.26	0.037	327.38	191.79	0.095

Results and Discussion

The cross-relaxation experiment (Figure 2), which relies upon the selective inversion of fluorine directly bonded to carbon-13, is dominated by the three parameters R_1^F, σ_{CF}, and R_1^C (which was determined from a separate experiment). Corresponding data (Figure 3) were fitted very satisfactorily by using eqs 1 restricted to a two-spin system in setting cross-correlation terms to zero. Influence of cross-correlation is negligibly small with respect to R_1^F and σ_{CF} even for long mixing times. At a field of 9.4 T, we obtain, with an accuracy that is believed to be better than 5%, the following results:

$$R_1^F = 0.198\ s^{-1} \quad \sigma_{CF} = 1.19 \times 10^{-2}\ s^{-1} \quad \text{and}$$
$$R_1^C = 3.30 \times 10^{-2}\ s^{-1}$$

It must be pointed out that R_1^F is the longitudinal relaxation rate of fluorine directly bonded to carbon-13. From the experiment sketched in Figure 4, the only reliable parameter that could be measured is the longitudinal relaxation rate of the two-spin order:

$$R_1^{CF} = 0.174\ s^{-1}$$

In the first cross-correlation experiment (Figure 6), the algebraic difference of the doublet intensities represents the buildup of the longitudinal spin order magnetization through the dipolar (^{13}C−^{19}F)−CSA(^{13}C) mechanism. The obtained curve (Figure 9) was fitted using eqs 1 in which $\sigma_{CSA(F),d}$ was set zero. This approximation is relevant because effects of this latter quantity should occur only at long mixing times. Taking into account the relative signs of the in-phase and antiphase components along with the phase cycling provides the sign of the cross-correlation rate;[1,4,29] we find

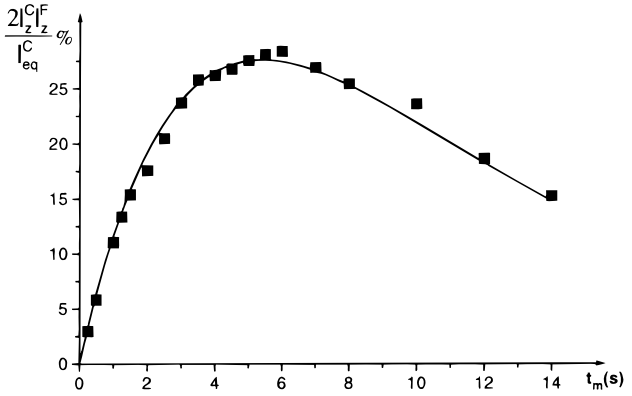

Figure 10. Build-up curve obtained by subtraction of the intensities of the two doublet components (data shown in Figure 8). The curve was fitted (solid line) according to eq 1 and yields the dipolar (^{19}F−^{13}C)-CSA(^{19}F) cross-correlation rate. Comparison with Figure 9 illustrates the larger effect of the CSA(^{19}F) mechanism.

$$\sigma_{CSA(C),d} = 6.66 \times 10^{-3}\ s^{-1}$$

From there one might go onto the second cross-correlation experiment (Figure 7), which is aimed at measuring the dipolar (^{13}C−^{19}F)−CSA(^{19}F) cross-correlation rate $\sigma_{CSA(F),d}$ as well as the ⟨⟨ nonselective ⟩⟩ cross-relaxation rate σ_{CF}^{ns} (the notation ns actually means that all fluorines have been perturbed). The algebraic sum of the carbon-13 doublet intensities (Figure 8) yields a build-up curve resulting from cross-relaxation interactions (data not shown), while their algebraic difference is associated with the creation of the longitudinal spin order via the dipolar (^{13}C−^{19}F)−CSA(^{13}C) term (Figure 10). Again cross-correlation data were fitted according to eqs 1, here without any restriction, and this leads to

$$\sigma_{CSA(F),d} = 3.72 \times 10^{-2}\ s^{-1}$$

Only the initial behavior of the cross-relaxation build-up curve was used to extract the nonselective cross-relaxation rate, which must be greater than the selective one

$$\sigma_{CF}^{ns} = 1.47 \times 10^{-2}\ s^{-1}$$

This is reminiscent of the results obtained in the case of benzene:[10] a non-negligible intermolecular dipolar contribution is the only way to explain the relatively important difference between selective and nonselective cross-relaxation rates. Then, the assumption of an isolated pair of spins in eqs 6 could be fulfilled by using the selective cross-relaxation rate, which depends solely on the two nucleus directly bonded. Finally, we have checked the consistency of our results by fitting again the whole experimental data set according to the full relaxation matrix.

Carbon-13 and flurorine-19 longitudinal relaxation rates have been measured with the help of different spectrometers as a function of the magnetic field B_0, and the resulting longitudinal relaxation rates are displayed in Figure 11. The linear slope with respect to B_0^2 is deduced from eq 6:

$$(2/15)(\gamma_X \Delta\sigma_X)^2 \tau_{CSA(X)} \qquad (9)$$

From all these measurements, it proves possible to extract the two correlation times $\tau_{||}$ and $\tau_{\perp}$ and the chemical shielding tensors. First, the assumption of an axial symmetry for the fluorine shielding tensor can be justified by the results of quantum chemistry calculations and the fact that the isotropic chemical shift remains unchanged between the solid and the

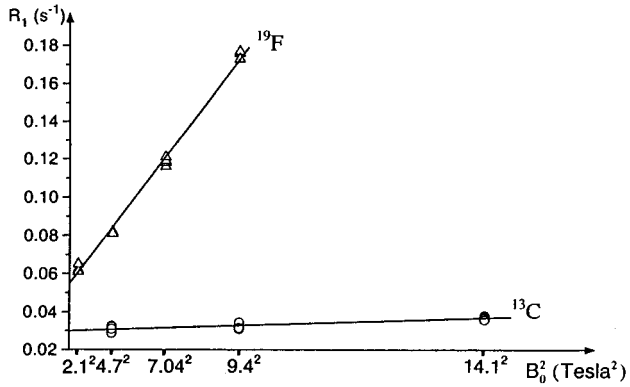

Figure 11. Linear behavior of carbon-13 and fluorine-19 longitudinal relaxation rates with respect to the square of the static magnetic field value (B_0^2). In order to increase the reliability of the carbon-13 data (so as to determine the relevant slope with a better accuracy), it was necessary to go to the highest field available and to repeat several times the measurements performed at each field.

TABLE 3: Chemical Shielding Tensor Parameters of Fluorine-19[a]

	solid-state NMR[33]	liquid-state NMR (this work)	quantum chemistry (this work)
σ_{xx}	299 ± 6	301.8 ± 7	257.4 to 279.5
σ_{yy}	299 ± 6	301.8 ± 7	269.5 to 286.0
σ_{zz}	457 ± 6	453.2 ± 7	453.5 to 460.9
isotropic shift (σ)	352	352.2	329.0 to 341.8
isotropic shift (δ)	−166.0	−166.3	−143.0 to −155.8
anisotropy $\Delta\sigma$	158.0	151.6	176.7 to 191.8
asymmetry η	0	0	0.04 to 0.16

[a] Chemical shifts (δ) are referred to trichlorofluoromethane. All data, except the dimensionless asymmetry parameter, are given in ppm.

liquid state agrees this hypothesis; it must be stressed that this axial symmetry is accidental. Now, setting $\eta_{CSA(F)} = 0$ in eqs 5′ and 7 and using a C−F bond length[30] of 1.33 Å, we are able to extract the three following parameters using eqs 2, 4′, and 6

$$\tau_\perp = 6.9 \pm 0.5 \text{ ps}$$

$$\tau_\parallel = 2.6 \pm 0.4 \text{ ps}$$

$$\Delta\sigma_F = 151.6 \pm 8 \text{ ppm}$$

Both correlation times are in good agreement with previous work.[31,32] Chemical shielding tensor elements could be easily derived from the isotropic fluorine chemical shift which has been measured relative to trichlorofluoromethane. Table 3 shows previous solid-state NMR results compared to those (experimental and calculated) obtained in this work. The assumption of an axially symmetric tensor for fluorine is fully justified as there is no significant difference between our results and those derived from solid-state NMR.[33,34] We can turn now to the main objective of this work, which is the determination of the carbon-13 shielding parameters. With the knowledge of $\tau_\perp$ it is possible to extract the chemical anisotropy and the asymmetry factor of carbon-13 from the variation of its longitudinal relaxation rate with respect to B_0^2 (eq 9) and from the value of the dipolar ($^{13}C-^{19}F$)-CSA(^{13}C) cross-relaxation rate at 9.4 T (eq 4). The chemical shielding parameters are summarized in Table 4. As is made clear by these results, the downfield isotropic shift of about 20 ppm in going from solid to liquid phases can be explained by the sole modification of the *z* shielding tensor component. Quantum chemistry calculations assuming an isolated molecule confirm nicely this trend.

TABLE 4: Chemical Shielding Tensor Parameters of Carbon-13[a]

	solid-state NMR[33] ($T = 233$ K)	liquid-state NMR (this work)	quantum chemistry (this work)
σ_{xx}	14 ± 6	8.4 ± 6	2.3 to 11.6
σ_{yy}	14 ± 6	22.6 ± 6	7.2 to 17.6
σ_{zz}	54 ± 8	106.9 ± 6	88.7 to 98.5
isotropic shift (σ scale)	27.3	45.9	34.1 to 40.9
isotropic shift (δ scale)	157.2	138.5	150.4 to 143.6
anisotropy $\Delta\sigma$	40	91.3 ± 5	81.9 to 87.9
asymmetry η	0	0.23 ± 0.1	0.01 to 0.19

[a] Chemical shifts (δ) are referred to TMS. All data, except the dimensionless asymmetry parameter, are given in ppm.

The little difference between the liquid- and the gas-phase (quantum chemistry calculations) tensors suggest that only a weak molecular complex formation could exist in the liquid state as determined experimentally in the case of benzene−hexafluorobenzene mixtures[31,35,36] and also suggested by other quantum calculations.[37] Comparing experimental data and theoretical results shows that a good agreement is reached for the carbon atom, although it is not clear which exchange-correlation functional of the electronic density reproduce the shielding tensor elements the best. If one look at GIAO and CSGI (or IGAIM) results, one can hardly select one method to be better than the other since they are doing as well (as bad) as the other. Absolute values concerning fluorine-19 are less satisfactory. Nevertheless, from a relative point of view, the maximal difference between the calculated values corresponds to about 10% of the mean value, thus not larger than for carbon. It is noteworthy that these calculations concern an isolated system and that the solvent bulk may have a non-negligible effect that could explain the discrepancy between theory and experiment. Calculations taking into account the electrostatic solvent effects are in progress.

Regarding the variation of the carbon-13 isotropic shift, we can adopt here the explanation proposed by Duer.[30] She has shown that the carbon-13 isotropic shift varies dramatically, in the same way, between pure solid hexafluorobenzene and a solid mixture 1:1 of benzene−hexafluorobenzene. Her explanation can be extended to the difference between the liquid and the solid state. In the solid state, it is known that two neighboring rings are approximately perpendicular to each other[38] with two fluorines of one ring pointing toward the ring of the other. These two fluorines will distort the π-electronic distribution in the ring and therefore give rise to the less shielding (i.e., an increase of the isotropic shift) in the solid state. This interaction completely vanishes in the liquid state even if molecular complexes exist as inferred from this work.

Conclusion

We have demonstrated that by using simple but judiciously chosen experimental NMR methods combined with quantum chemistry calculations, it is possible to determine the chemical shielding tensor in the liquid state even in the case of a complicated spin system. Modifications of the electronic distribution around the carbon nuclei in hexafluorobenzene when going from pure solid to pure liquid or solutions can be satisfactorily explained by the particular arrangement in the solid phase.

Acknowledgment. We are most grateful to Prof. Jacques Reisse, Dr. Kristin Bartik, and Mr. M. Luhmer for the use of the Varian 600 MHz spectrometer at Université Libre de Bruxelles.

References and Notes

(1) Werbelow, L. G.; Grant, D. M. *Adv. Magn. Reson.* **1977**, *9*, 189.
(2) Vold, R. L.; Vold, R. R. *Prog. Nucl. Magn. Reson. Spectrosc.* **1978**, 79.
(3) Goldman, M. *J. Magn. Reson.* **1984**, *60*, 437.
(4) Jaccard, G.; Wimperis, S.; Bodenhausen, G. *Chem. Phys. Lett.* **1987**, *138*, 601.
(5) Königsberger, E.; Sterk, H. *J. Chem. Phys.* **1985**, *83*, 2723.
(6) Burghardt, I.; Konrat, R.; Bodenhausen, G. *Mol. Phys.* **1992**, *75*, 467.
(7) Mäler, L.; Kowaleski, J. *Chem. Phys. Lett.* **1992**, *5*, 595.
(8) Tjandra, N.; Bax, A. *J. Am. Chem. Soc.* **1997**, *119*, 8076.
(9) Tessari, M.; Vis, H.; Boelens, R.; Kaptein, R.; Vuister, G. W. *J. Am. Chem. Soc.* **1997**, *119*, 8985.
(10) Python, H.; Mutzenhardt, P.; Canet, D. *J. Phys. Chem.* **1997**, *101*, 1793.
(11) Canet, D. In *NMR concepts and methods*; Wiley: New York, 1996.
(12) Markley, J. L.; Horsley, W. J.; Klein, M. P. *J. Chem. Phys.* **1971**, *55*, 3604.
(13) Canet, D.; Levy, G. C.; Peat, I. R. *J. Magn. Reson.* **1975**, *18*, 199.
(14) Canet, D.; Brondeau, J.; Elbayed, K. *J. Magn. Reson.* **1988**, *77*, 483.
(15) Furo, I.; Mutzenhardt, P.; Canet, D. *J. Am. Chem. Soc.* **1995**, *117*, 10405.
(16) Emetarom, C.; Hwang, T. L.; Mackin, G.; Shaka, A. J. *J. Magn. Reson.* **1995**, *A115*, 137.
(17) Canet, D. *Prog. Nucl. Magn. Reson. Spectrosc.* **1997**, *30*, 101.
(18) Tossell, J. A. *Nuclear Magnetic Shieldings and Molecular Structure*; Kluwer Academics: Dordrecht, 1993.
(19) Cybulski, S. M.; Bishop, D. M. *J. Chem. Phys.* **1993**, *98*, 8057.
(20) Woon, D. F.; Dunning, T. H., Jr. *J. Chem. Phys.* **1993**, *98*, 1358.
(21) Becke, A. D. *Phys. Rev. A* **1988**, *38*, 3098.
(22) Becke, A. D. *Chem. Phys.* **1993**, *98*, 5648.
(23) Lee, C.; Yang, W.; Parr, R. G. *Phys. Rev. B* **1988**, *37*, 785.
(24) Perdew, J. P.; Wang, Y. *Phys. Rev. B* **1992**, *45*, 13244.
(25) Ditchfield, R. *Mol. Phys.* **1974**, *27*, 789.
(26) Gauss, J. *J. Chem. Phys.* **1993**, *99*, 3629.
(27) Keith, T. A.; Bader, R. F. W. *Chem. Phys. Lett.* **1992**, *194*, 1.
(28) Frisch, M. J.; Trucks, G. W.; Schlegel, H. B.; Gill, P. M. W.; Johnson, B. G.; Robb, M. A.; Cheeseman, J. R.; Keith, T.; Petersson, G. A.; Montgomery, J. A.; Raghavachari, K.; Al-Laham, M. A.; Zakrzewski, V. G.; Ortiz, J. V.; Foresman, J. B.; Peng, C. Y.; Ayala, P. Y.; Chen, W.; Wong, M. W.; Andres, J. L.; Replogle, E. S.; Gomperts, R.; Martin, R. L.; Fox, D. J.; Binkley, J. S.; Defrees, D. J.; Baker, J.; Stewart, J. P.; Head-Gordon, M.; Gonzalez, C.; Pople, J. A. *Gaussian*; Gaussian Inc.: Pittsburgh PA, 1995.
(29) Sorensen, O. W.; Eich, G. W.; Levitt, M. H.; Bodenhausen, G.; Ernst, R. R. *Prog. Nucl. Magn. Reson. Spectrosc.* **1983**, *16*, 163.
(30) Duer, M. J. *J. Chem. Soc., Faraday Trans.* **1993**, *89*, 823.
(31) Suhm, M. A.; Müller, K. J.; Weingärtner, H. Z. *Phys. Chem., Neue Folge* **1987**, *155*, 101.
(32) Suhm, M. A.; Weingärtner, H. *Chem. Phys. Lett.* **1989**, *159*, 193.
(33) Pines, A.; Gibby, M. G.; Waugh, J. S. *Chem. Phys. Lett.* **1972**, *15*, 373.
(34) Raber, H.; Mehring, M. *Chem. Phys.* **1977**, *26*, 123.
(35) Neelakandan, M.; Pant, D.; Quitevis, A. L. *Chem. Phys. Lett.* **1997**, *265*, 283.
(36) Laatikainen, R.; Santa, H.; Hiltunen, Y.; Lounila, J. *J. Magn. Reson.* **1993**, *A104*, 238.
(37) Hernandez, J.; Colmenares, F.; Cuevas, G.; Costas, M. *Chem. Phys. Lett.* **1997**, *265*, 503.
(38) Boden, N.; Davis, P. P. *Mol. Phys.* **1973**, *25*, 81.